

# Measurement method of the relative propagation delay of two signals based on modified caliper ruler

Hon-Tung Luk\* and Lian-Kuan Chen

Department of Information Engineering, The Chinese University of Hong Kong, Hong Kong, China

\*Corresponding author: lht010@ie.cuhk.edu.hk

Received July 23, 2013; revised October 3, 2013; accepted October 4, 2013;

posted October 7, 2013 (Doc. ID 194319); published November 8, 2013

A novel measurement technique for the relative propagation delay of two signals based on a caliper ruler is proposed. The technique is applied to the chromatic dispersion measurements of single-mode fiber (SMF), dispersion-compensation fiber, and dispersion-shifted fiber. Compared to the conventional time-of-flight method, dispersion can be measured even when the delay difference is smaller than the measurement pulse's width. The sign of dispersion is preserved during measurement. The scheme also supports the usage of multiple wavelengths simultaneously for fast measurement. Measurement error of less than 0.2 ps/(km \* nm) in SMF is experimentally demonstrated. © 2013 Optical Society of America

OCIS codes: (060.2270) Fiber characterization; (060.2300) Fiber measurements; (260.2030) Dispersion.

<http://dx.doi.org/10.1364/OL.38.004659>

Measurement of the relative delay of two signals is essential for many applications to characterize a transmission channel. For instance, chromatic dispersion of a fiber can be obtained from the relative delay of two signals of different wavelengths. The commonly used dispersion measurement methods are the time-of-flight method and the phase-shift method [1]. For the time-of-flight method, short pulses are generated at different wavelengths and launched into the test fiber at the same time. Chromatic dispersion is measured by the relative delays of arrival times between two wavelengths. This method requires extremely accurate arrival time measurement and short pulsewidth as the pulses of different wavelengths need to be separated at least a pulsewidth in time for differentiation [2]. The phase-shift method is realized by modulating the light sources with a sinusoidal signal and then estimating the dispersion-induced relative phase shift at the receiver. This method is cost-effective and is one of the most widely used methods in current measurement systems [3,4]. In the measurement of small dispersion values, the interferometric method is suitable for measuring short fiber sections [5]. The light source is split into two arms and recombined again. The interference between the tunable reference arm and the test fiber arm provides an accurate measurement of dispersion for fiber less than 1 m. Dispersion monitoring by detecting the changes of RF clock tone power has also been proposed [6]. However, the sign of dispersion cannot be determined. Nonlinear methods have also been proposed and show the capability of measuring higher-order dispersion [7,8]. To release the limitation of measurement range of the interferometric method and overcome the problem of a delay difference smaller than the pulsewidth, we propose a novel scheme for dispersion measurement by calculating time alignment shifting of two pulse trains at different wavelengths with slightly different time periods, which is called the *time caliper method*. The principle of this method is similar to the Vernier caliper for distance measurement [9]. The proposed scheme is capable of measuring a large dispersion range as well as maintaining relatively high accuracy. Only a single receiver is required for simultaneous measurement of

relative delays among multiple wavelength channels. Demultiplexing is not required for the proper operation of the scheme. The scheme can be extended to the characterization of different multiplexing channels, such as polarization division multiplexing and space division multiplexing.

Chromatic dispersion is caused by the propagation speed differences between different wavelengths in fiber. Without loss of generality, we consider the dispersion between two wavelengths,  $\lambda_1$  and  $\lambda_2$ . The measurement system setup is shown in Fig. 1. A repeating pulse train of period  $T$  at wavelength  $\lambda_1$  is launched into the test fiber through a coupler. Simultaneously, a second pulse train at wavelength  $\lambda_2$  of a slightly shorter repeating period,  $T - \delta$ , is coupled into the test fiber. For convenience,  $\delta$  is chosen as a submultiple of  $T$ . The combined signal is detected at the receiver and displayed on the oscilloscope. When pulses from the two wavelengths arrive with overlap in time, their intensities are added. Suppose the pulses in the two pulse trains are of the same

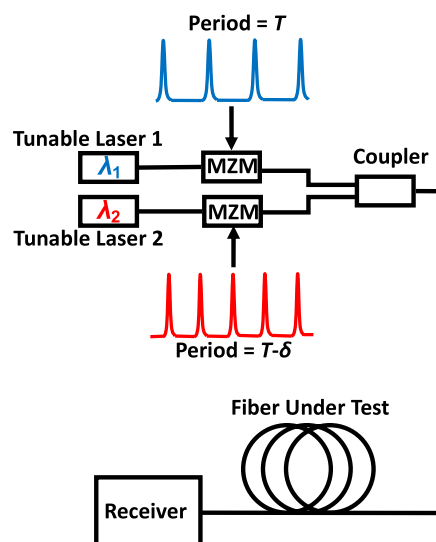


Fig. 1. Schematic diagram of the proposed measurement system.

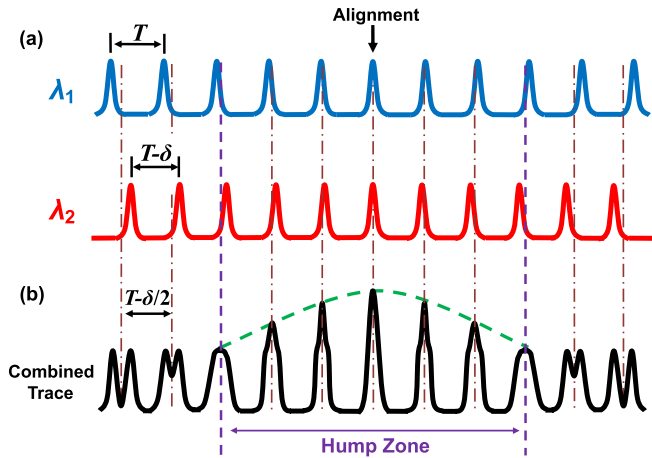


Fig. 2. (a) Time domain traces of the pulse trains of two wavelengths. (b) Combined trace in back-to-back transmission. The green dashed line is the envelope of the peak intensity in the hump zone. The grid is aligned with the midpoint between two overlapped pulses.

pulse shape and the full width half-maximum pulsewidth is  $w$ . When the separation of the two overlapped pulses, defined as  $x$ , is larger than  $w$ , the combined pulse's peak intensity will not be larger than that of the original pulses. The duration that the combined pulses' intensity is larger than that of the original pulses is defined as the *hump zone*, as shown in Fig. 2(b). First we obtain a reference trace by measuring the combined trace in back-to-back transmission. After transmission in the fiber under test, dispersion will cause a shifting of the time alignment between the two pulse trains, shown as a shifting of the hump zone at the receiver. The dispersion value can be derived from the amount of shifting compared with the reference trace.

The proposed scheme scales the small time shift of the two pulse trains, due to dispersion, to a large time shift of the hump zone. The scaling factor can be derived in the following, similar to the Vernier scale in caliper ruler [9], and is found to be  $(T - \delta/2)/\delta$ . Figure 3(a) shows a closer look at a pair of overlapped pulses in the hump zone with  $x < w$ . The intensity of the midpoint  $M$  between the two pulses is a function of  $x$ , defined as  $f(x)$ , as plotted in Fig. 3(b). For symmetric pulses,  $f(x)$  corresponds to the peak intensities of the combined pulses.  $f(x)$  exhibits

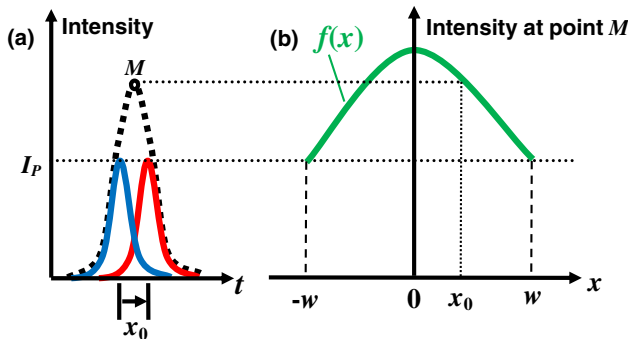


Fig. 3. (a) Pulses from the two pulse trains are overlapped with separation  $x_0$ . (b) Added intensity at the midpoint  $M$  between two pulses versus separation  $x$ .

the same shape as the envelope of the hump zone in Fig. 2(b), with the only difference in the horizontal axis. Note that the separation of pulses in the hump zone takes a sequence of discrete values with step size of  $\delta$ , which corresponds to a scaling of  $1/\delta$  to the horizontal axis of  $f(x)$ . The time separation between adjacent pairs of overlapped pulses is  $(T - \delta/2)$ , as shown by the grid in Fig. 2(b). This indicates a scaling of  $(T - \delta/2)$  to the horizontal axis of  $f(x)$ . Thus the scaling factor of the horizontal axis is  $(T - \delta/2)/\delta$  and the envelope of the hump zone can be derived. The scaling factor states that for each time shifting of  $(T - \delta/2)$  of the hump zone, the corresponding dispersion value is  $\delta$ .

A period equal to  $T((T/\delta) - 1)$  of the combined trace centered at the hump zone is selected for the derivation of dispersion. An empty marker equal to  $3T$  is inserted at the beginning of this period as a stationary reference. For easy illustration of the concept, we number the pulses starting from the marker as shown in Fig. 4. In the following we will give examples and discuss a few measurement issues.

To evaluate the time shift, we consider the maximum intensity pulse in the hump zones before and after transmission. If the index number of the maximum intensity pulse is changed by  $m$ , which corresponds to a shifting of  $m(T - \delta/2)$  according to the grid, the propagation delay difference  $\tau$  of the two wavelengths is estimated to be  $m\delta$  according to the scaling factor derived before. For example, in Fig. 4(b) the measured propagation delay difference  $\tau$  is  $7\delta$  when the index number of the maximum intensity pulse is changed from 6 to 13. This is similar to the derivation of the Vernier scale of the Vernier caliper for length measurement [9].

The envelope connecting the peak intensity of all pulses in the hump zone is shown as the dashed curve in Fig. 4. Note that the maximum intensity pulse in the hump zone may not be located right in the middle of the zone, as illustrated in Fig. 4(c). Taking the maximum

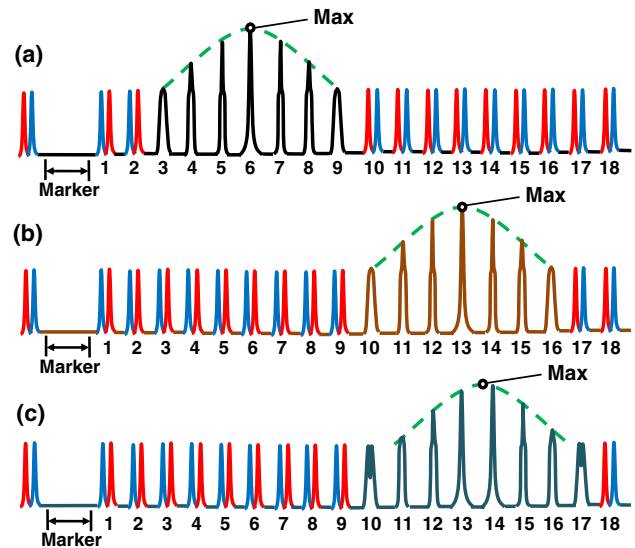


Fig. 4. (a) Reference trace. (b) After transmission, the maximum intensity pulse locates at the middle of the envelope. (c) After transmission, the maximum intensity pulse is not at the middle of the envelope.

intensity pulse for the measurement of pulse shifting will not be accurate in this case. One solution is to correlate the reference intensity envelope in Fig. 4(a) with the measured combined trace in Fig. 4(c). When the correlation achieves maximum, the envelope is fitted to the trace. Suppose the maximum point of the envelope is located between  $m(T - \delta/2)$  and  $(m + 1)(T - \delta/2)$  shifting according to the grid; the propagation delay difference is the linear interpolation between  $m\delta$  and  $(m + 1)\delta$ , according to the time delay of the maximum point. This interpolation feature is a refinement of the caliper method. For example, in Fig. 4(c), the maximum point is at two thirds between the 13th and 14th pulses. The propagation delay difference  $\tau$  is derived as  $7.67\delta$ . The dispersion value at  $\lambda$ , equal to  $(\lambda_1 + \lambda_2)/2$ , can be derived by

$$D(\lambda) = \frac{\tau}{L(\lambda_2 - \lambda_1)}, \quad (1)$$

where  $L$  is the length of the fiber under test.

To determine the sign of dispersion, we consider the case in single-mode fiber (SMF). Let  $\lambda_{ZD}$  be the zero dispersion wavelength. If  $\lambda_2 > \lambda_1 > \lambda_{ZD}$ ,  $\lambda_2$  travels slower than  $\lambda_1$ . The hump zone is shifted to the right. If  $\lambda_{ZD} > \lambda_2 > \lambda_1$ ,  $\lambda_2$  travels faster than  $\lambda_1$ . The hump zone is shifted to the left. From the direction of the shifting, we can easily determine the sign of the dispersion.

The scheme works for arbitrary symmetric pulse shape. It can be shown that to ensure there is always a hump zone in each period,  $w > \delta/2$  is required. Actually there are  $2w/\delta$  pulses in the hump zone, resulting from overlaying of two pulse trains. For a large  $w$  and a small  $\delta$ , the hump zone can last for a longer time.

Note that the resolution of the time-of-flight method is limited by the dispersion-induced pulse broadening effect due to its requirement of accurate arrival time measurement. On the other hand, the resolution of this proposed scheme depends on  $\delta$ . The pulsewidth can be much larger than  $\delta$  (up to 10 times in our experiment). Thus this scheme is robust to the pulse broadening effect by dispersion.

Conventionally, one period of the combined trace is taken centered at the hump zone for analysis. Since the combined pulse train is periodic, the intensity noise can be reduced by averaging multiple periods of the combined trace.

In the following we will discuss a few possible extensions of our proposed scheme. To achieve fast dispersion measurement, multiple wavelength sources modulated with slightly different frequencies can be launched into the fiber for simultaneous measurement. Several schemes have been proposed to realize a multiwavelength mode lock laser for multiwavelength pulse generation [10,11]. Very accurate measurements, even on short samples of fibers, could be made by using higher repetition rate mode locked fiber lasers with small difference of repetition frequencies. The commercially available mode locked lasers can provide 10 GHz pulses with only a few picoseconds of delay.

Even though there are multiple wavelengths launched into the fiber, the repetition rate of the hump zone can be different for different combinations of wavelengths.

The repetition rate depends on the periods of the pulse trains modulated on the two wavelengths. For example, consider three wavelengths  $\lambda_1$ ,  $\lambda_2$ , and  $\lambda_3$  under the case of back-to-back transmission as illustrated in Fig. 5. Suppose the periods of the pulse trains modulated on  $\lambda_1$ ,  $\lambda_2$ , and  $\lambda_3$  are  $T_1 = 61\delta$ ,  $T_2 = 60\delta$ , and  $T_3 = 59\delta$ , respectively. The period of the hump zone between  $\lambda_1$  and  $\lambda_2$  is  $T_1T_2/\delta$ . It is easy to select a time region in which the hump zone is obtained only by overlapping the pulses from  $\lambda_1$  and  $\lambda_2$  when analyzing the delay difference between  $\lambda_1$  and  $\lambda_2$ . Suppose the pulses from all wavelengths are aligned at  $t = 0$ . For example, after 20 repetitions of hump zones, the hump zones are centered at  $t = 73200\delta$ ,  $71980\delta$ , and  $70800\delta$  for (a)  $\lambda_1$  and  $\lambda_2$ , (b)  $\lambda_1$  and  $\lambda_3$ , and (c)  $\lambda_2$  and  $\lambda_3$ , respectively, as shown in Fig. 5.

On the other hand, if cost is an issue, an extension of the proposed scheme to a single tunable laser case with a single modulator is possible by capturing and processing the waveforms at the receiver. This has been experimentally demonstrated but is not presented here due the limited space.

Next we will show the experimental results with a setup similar to that in Fig. 1. Two tunable distributed feedback (DFB) lasers at  $\lambda_1$  and  $\lambda_2$  are employed as the sources to estimate the dispersion at  $(\lambda_1 + \lambda_2)/2$ .  $\lambda_1$  and  $\lambda_2$  can be tuned within the range from 1500 to 1600 nm. The two pulse trains can be generated by the two outputs from an arbitrary waveform generator. To obtain high-resolution dispersion measurement,  $\delta$  is set to be 100 ps.  $T$  is set to be 40 ns so that the measurement range of propagation delay difference is  $\pm 20$  ns. The empty marker lasts for 120 ns. The launching peak power is kept below  $-7$  dBm to maintain operation in the linear regime. Dispersion measurement has been performed on a 50 km standard SMF, a 10 km dispersion-shifted fiber (DSF), and a 2.8 km dispersion-compensation fiber (DCF).

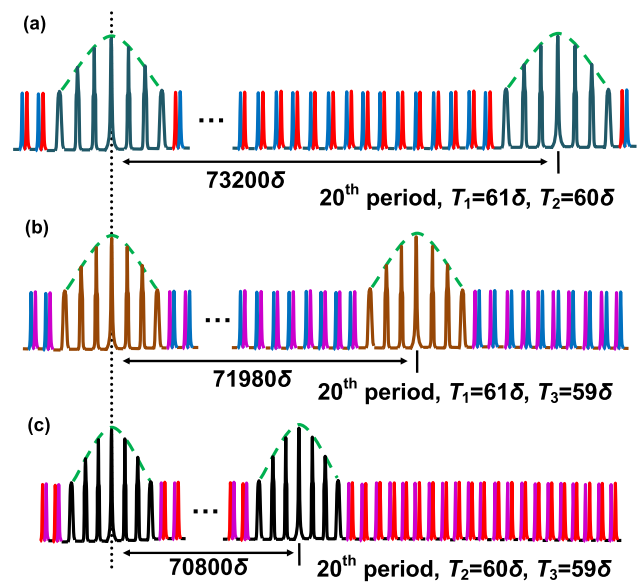


Fig. 5. Humps occur at different times due to the periods of humps being different. The time delays of the 20th hump counted from the aligned pulse are (a)  $73200\delta$  for  $\lambda_1$  and  $\lambda_2$ , (b)  $71980\delta$  for  $\lambda_1$  and  $\lambda_3$ , and (c)  $70800\delta$  for  $\lambda_2$  and  $\lambda_3$ .

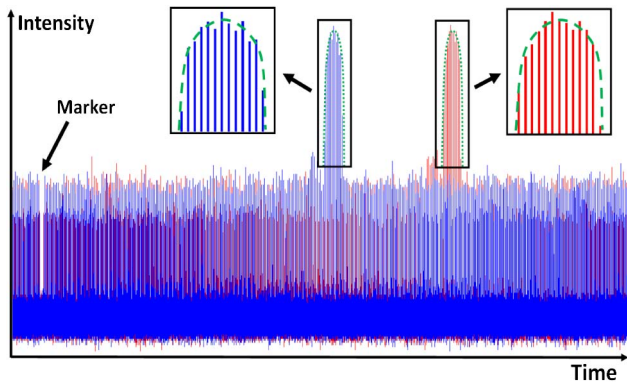


Fig. 6. Reference trace with zero dispersion (blue) and the measured trace after 50 km SMF transmission (red) with wavelengths of 1540 and 1550 nm.

Figure 6 shows the reference trace of zero dispersion (blue) and the measured trace after 50 km SMF transmission (red) with  $\lambda_1 = 1540$  nm and  $\lambda_2 = 1550$  nm, and the pulsewidth  $w$  is 500 ps. The hump zone is shifted to the right. The arrival time delay between the two wavelengths is derived to be 7.98 ns by estimating the time shifting. Thus the measured dispersion coefficient of SMF at  $\lambda = 1545$  nm is 15.96 ps/(km \* nm).

By tuning the central wavelengths of both lasers, we can measure the dispersion of the fiber over different wavelengths, and the third-order dispersion can also be derived. Figure 7 shows the measured dispersion curves versus the wavelength of the 50 km SMF, 10 km DSF, and 2.8 km DCF. The curves match with the standard SMF, DSF, and DCF dispersion curves. The measured dispersion coefficient of SMF ranges from 14.3 ps/(km \* nm) at 1515 nm to 18.3 ps/(km \* nm) at 1585 nm. The values of the dispersion coefficient agree with the empirical formula of chromatic dispersion derived from the Sellmeier equation with zero dispersion wavelength at 1310 and dispersion characteristics slope of 0.09 ps/(km \* nm<sup>2</sup>) [12]. The sign of dispersion is preserved in the measurement of DSF. The accuracy is relatively high even when the measuring wavelength is close to the zero dispersion wavelength of the fiber. The zero dispersion wavelength is at 1548 nm, and the dispersion slope is 0.08 ps/(km \* nm<sup>2</sup>). The measurement result of DCF shows that the proposed method

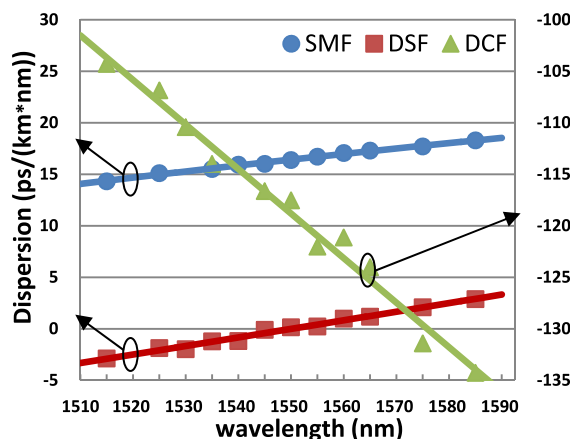


Fig. 7. Measured dispersion plot versus wavelength.

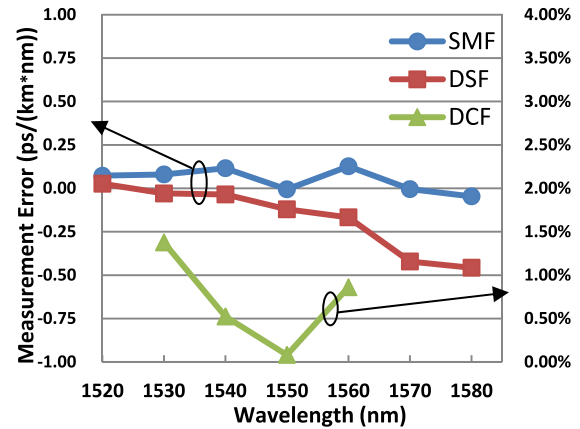


Fig. 8. Measurement error versus wavelength.

is also capable of measuring fibers with large dispersion values.

Figure 8 shows the measurement error (for SMF and DSF) and error percentage (for DCF) compared to the measurements by commercial optical time-domain reflectometer (OTDR). The measurement error is less than 0.2 ps/(km \* nm) for SMF and less than 0.5 ps/(km \* nm) for DSF. For DCF, which has much larger dispersion, the error percentage is less than 2% of the absolute dispersion value.

In conclusion, we have proposed and demonstrated a novel dispersion measurement scheme with a large measurement range and relatively high accuracy. The scheme preserves the sign of the dispersion and is robust to the pulse broadening effect. The humps in multiwavelength measurement can be easily separated for the derivation of dispersion at different wavelengths simultaneously. The measurement error compared to that by commercial OTDR is less than 0.2 ps/(km \* nm) in SMF.

This work is supported in part by HKSAR RGC GRF 410910. The authors thank Dr. Kam-Hon Tse for advice regarding the experimental demonstration.

## References

1. L. G. Cohen, *J. Lightwave Technol.* **3**, 958 (1985).
2. C. Lin, A. R. Tynes, A. Tomita, P. L. Liu, and D. L. Philen, *Bell Syst. Tech. J.* **62**, 457 (1983).
3. B. Costa, D. Mazzoni, M. Puleo, and E. Vezzoni, *IEEE Trans. Microwave Theor. Tech.* **MTT-30**, 1509 (1982).
4. C. Yu, G. J. Pendock, X. Yi, and W. Shieh, in *Proceedings of the Optical Fiber Communication Conference and Exposition and the National Fiber Optic Engineers Conference* (2008), paper JWA29.
5. P. Merritt, R. P. Tatam, and D. A. Jackson, *J. Lightwave Technol.* **7**, 703 (1989).
6. G.-W. Lu, K. T. Tsai, W. I. Way, and L.-K. Chen, in *Proceedings of the European Conference and Exhibition on Optical Communication* (2006), paper We3.P.67.
7. J. Fatome, S. Pitois, and G. Millot, *Opt. Fiber Technol.* **12**, 243 (2006).
8. H. Chen, *Opt. Commun.* **220**, 331 (2003).
9. [http://en.wikipedia.org/wiki/Vernier\\_scale](http://en.wikipedia.org/wiki/Vernier_scale).
10. D. Chen, C. Shu, and S. He, *Opt. Lett.*, **33**, 1395 (2008).
11. X. Li, J. Yu, Z. Dong, J. Zhang, Y. Shao, and N. Chi, *Opt. Express* **20**, 21833 (2012).
12. Corning Incorporated, Single-Mode Dispersion Measurement Method, MM26 (2001).